

# Mental States, EEG Manifestations, and Mentally Emulated Digital Circuits for Brain-Robot Interaction

Stevo Bozinovski, *Senior Member, IEEE*, and Adrijan Bozinovski, *Member, IEEE*

**Abstract**—This paper focuses on electroencephalogram (EEG) manifestations of mental states and actions, emulation of control and communication structures using EEG manifestations, and their application in brain-robot interactions. The paper introduces a mentally emulated demultiplexer, a device which uses mental actions to demultiplex a single EEG channel into multiple digital commands. The presented device is applicable in controlling several objects through a single EEG channel. The experimental proof of the concept is given by an obstacle-containing trajectory which should be negotiated by a robotic arm with two degrees of freedom, controlled by mental states of a human brain using a single EEG channel. The work is presented in the framework of Human-Robot interaction (HRI), specifically in the framework of brain-robot interaction (BRI). This work is a continuation of a previous work on developing mentally emulated digital devices, such as a mental action switch, and a mental states flip-flop.

**Index Terms**—Brain-robot interaction (BRI), electroencephalogram (EEG) manifestations of mental states and actions, mental action EEG switch, mental state CNV flip-flop, mentally emulated EEG demultiplexer.

## I. INTRODUCTION

**M**ENTAL actions are important in the study of mental activity and development, but there is a feeling that “... despite the fact that it should be at the centre of the philosophy of mind, the topic of mental action has been somewhat overlooked.” [1] In this work, we are interested in *mental states and actions as electrophysiologically visible phenomena of the mind and mental development*. Here the term “mental” refers to the cognitive, behavioral, and other mental skills exhibited by humans, higher animals, and artificially “intelligent” systems [2]. A mental action is understood as an action of a human mind and/or human brain that changes a mental state. A mental state is understood inductively as an element of a set of states such as {relaxation, alertness, expectation, attention, . . . stateN}, where stateN just denotes an assumption that this set is finite. The type of a state can be emotional, motivational, or another type. An example of a mental action is changing a state of relaxation into

a state of attention. Another example is the change of a state of expectation into a state of nonexpectation. Mental states and actions are parts of the autonomous mental development. That term refers to the computational process by which a brain-like machine, natural or artificial, autonomously develops mental skills [2]. In robotics, a mental function is related to internal representation of the external world, and mental ability is related to the perception-decision-action loop [3].

In humans, mental states and their changes have various manifestations, *one of them being a manifestation in the electromagnetic energy emanating from the brain*. It has been pointed out that electromagnetic energy can be used for assessment of mental energy [4].

The electroencephalogram (EEG) is a tool used to represent a manifestation of the energy emanating from particular spot(s) of the human scalp, the scalp being outside the brain. An EEG also manifests mental states and their changes. An example of an EEG manifestation of a mental state is the Contingent Negative Variation (CNV) potential [5] which manifests a mental state of expectation. Another example is the amplitude of an EEG alpha rhythm [6]. The alpha rhythm is the prominent EEG wave pattern of an adult who is awake but relaxed with eyes closed. Some subjects trained in relaxation techniques can maintain high alpha amplitudes even with their eyes open [7]. Also, the alpha rhythm measured from the motor area (named mu rhythm) has higher amplitude when no motor activity (real, imaginary, or intentional) is undertaken. Thus, the alpha rhythm is used as a manifestation of a state of wakeful rest of the brain, but its role is not just a messenger of such a state (e.g., [8]). The alpha rhythm is also used as a measure of autonomous mental development in humans, in relation to electrical maturity of the brain. There is no dominant occipital activity before the age of 3 mo, at which time a rhythm of 3–4 Hz can be seen. The dominant frequency increases to approximately 5 Hz at age 6 mo, a 6–7 Hz rhythm is prevalent from 9 to 18 mo, by the age of 2 a 7–8 Hz rhythm is seen, which increases to 9 Hz by the age of 7, and at the age of 15 the alpha rhythm is developed with the frequency around 10 Hz [9].

Using the concepts of mental states and mental actions, this work considers mental constructs like mentally emulated digital circuits. Here, a mentally emulated digital circuit is understood as an emulation of the work of a digital control circuit, where the input signals are EEG signals. Three types of mentally emulated digital circuits will be discussed: a mental action switch, a mental state flip-flop, and a mental action demultiplexer.

The motivations for this work are:

- 1) “Understanding by building” is a way of research in embodied Artificial Intelligence (e.g., [10]). It is believed that

Manuscript received August 17, 2014; revised November 16, 2014; accepted December 24, 2014. Date of publication February 10, 2015; date of current version March 11, 2015. This work was supported in part by the NSF under Grant EPS-0447660-2005-701 to South Carolina State University.

S. Bozinovski is with the Department of Mathematics and Computer Science, South Carolina State University, Orangeburg, SC 29117 USA, and also with the Faculty of Computer Sciences and Engineering, Sts. Cyril and Methodius University, Skopje 1000, Macedonia (e-mail: sbozinovski@scsu.edu).

A. Bozinovski is with the School of Computer Science and Information Technology, University American College Skopje, Skopje 1000, Macedonia (e-mail: bozinovski@uacs.edu.mk).

Color versions of one or more of the figures in this paper are available online at <http://ieeexplore.ieee.org>.

Digital Object Identifier 10.1109/TAMD.2014.2387271

by building mentally emulated digital circuits, one can obtain better understanding of mental states and actions, and autonomous mental development in general.

- 2) Building mental structures, which emulate the work of control and communication circuits, such as switch, flip-flop, and demultiplexer, to be used in control of physical devices such as robots.
- 3) Application of the mental control structures in various applications of Brain-Robot Interaction, which is viewed as a part of a wider field of Human–Robot Interaction (HRI) [11].
- 4) Building BRI devices where a single EEG channel will be able to carry multiple commands to robot(s). The EEG demultiplexer proposed here is a solution in that direction.

Besides robots, other objects (both physical and virtual) in the environment surrounding a human subject can also be controlled using these devices, which is in the scope of the field of Brain-Computer Interface (BCI), the term proposed in [12]. There is a belief in the field of applications of BCI products that approach based on a low number of channels will play a key role in the application of mind-controlled devices (e.g., [13]). Products with a low number of channels, especially single-channel EEG products, have been of special interest in BCI applications. An example of a single-channel commercially available device is the Brain Wave Mobile, from Neurosky, Inc. [14]. Single-channel devices are used in applications such as EEG based biometrics [15]. Currently a solution exists for using a single audio channel of a laptop as an EEG channel [16]. Computer games based on the relaxation state have been of interest [17].

Driven by these motives and the context, in this paper we present the idea, and experimental proof-of-the-concept, of a mentally emulated EEG demultiplexer. In developing methods for building an EEG demultiplexer, we also present a view of an *EEG modem*, and a view that the alpha rhythm is an amplitude modulation (AM) of the message to be sent over an EEG channel.

The following text is organized in 13 sections. After this introduction which relates the paper to mental states, actions, and mentally emulated digital circuits, the paper gives the description of Brain-Robot Interaction as an Autonomous Mental Development paradigm. Then it describes previously proposed mentally emulated digital circuits, namely the EEG switch and the CNV flip-flop. Then it gives a background of the concept of a demultiplexer and a redundant demultiplexer. Section V introduces the mentally emulated EEG demultiplexer and gives its formal description. The realization of such a concept is given in the next section. Section VII describes the demonstration scenario for the proof-of-the-concept experiments. Section VIII describes the realization methods, which are then used in the implementation software described in Section IX. Section X describes the experimental investigation. Results and the proof of the concept are presented in Section XI, where also an application of the proposed EEG demultiplexer beyond the proof of the concept is mentioned. A separate section is provided for discussion. The last is the conclusion section.

## II. BRAIN–ROBOT INTERACTION AS AN AUTONOMOUS MENTAL DEVELOPMENT PARADIGM

A Brain-Robot Interaction (BRI) setup [18], [19] is usually viewed as a BCI setup. The BCI concept is based on a computer

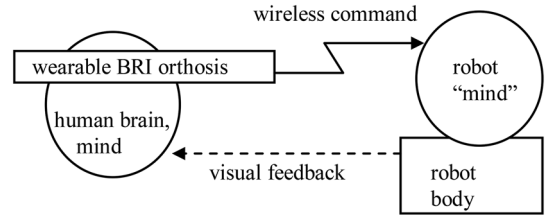


Fig. 1. Brain-Robot Interaction setup.

as the central part of the scenario. It is also considered within the general framework of biological signal processing [20]. So in a BRI, a computer receives EEG signals, recognizes the feature in the signals which can be interpreted as a control switch generated by a human brain, and controls a robot behavior accordingly. However, current technology lets the computer be seen either as a part of the EEG-to-robot interface or as a part of the robot itself. So, a BRI setup can be shown as in Fig. 1.

Fig. 1 shows a BRI-based on a *wearable orthosis* (e.g., some kind of eye glasses), which contains a microprocessor based artificial intelligence system, able to perform at least some EEG pattern recognition, based on Machine Learning. So, the computer is a part of the BRI orthosis and is not emphasized in the BRI setup. The computer screen can be generated on the orthotic eye glasses if needed. The artificial intelligence system which will develop skills to understand EEG signals can be viewed as a computational mental development system, and in some applications it will be autonomous. The human brain involved is an autonomous mental development system which will develop a skill to communicate with a robot using its own mental faculties and its own EEG signals. Let us note that the BRI orthosis in Fig. 1 could also use other brain signals, such as functional near-infrared spectroscopy [11].

### A. EEG Manifestations of Mental States

EEG manifestations of mental states are usually divided into rhythms of spontaneous EEG signals and event related potentials in the EEG signals. Fig. 2 shows a taxonomy of brain potentials [21].

As can be seen from Fig. 2, the spontaneous potentials are represented by frequency bands (rhythms). They represent various states of the brain such as sleep, relaxation, alertness etc. An example of an EEG rhythm is the EEG alpha rhythm, a signal composed of the EEG frequency band 8-13 Hz. We denote a change of the amplitudes of the alpha rhythm, due to mental action, as Contingent Alpha Variation (C $\alpha$ V). The event related potentials are further divided into preevent and postevent. The postevent, or evoked, potentials can be reflexive (exogenous) such as the Visual Evoked Potential (VEP), or cognitive or endogenous, such as the P300 potential. The P300 represents a state of recognition. An example of a preevent or anticipatory potential is the contingent negative variation (CNV) potential. In order to appear in the brain, a CNV potential requires *development of an expectation state*. It is a learning process in which the brain realizes that there is a stimulus from the environment that should be expected [4]. An example of a preparatory preevent potential is the Bereitschaftspotential (BP), which represents a state of readiness for some action.

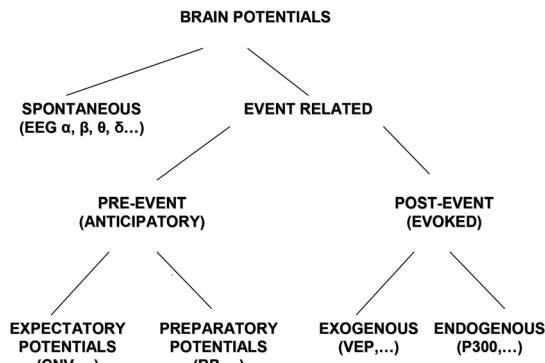


Fig. 2. Taxonomy of brain potentials.

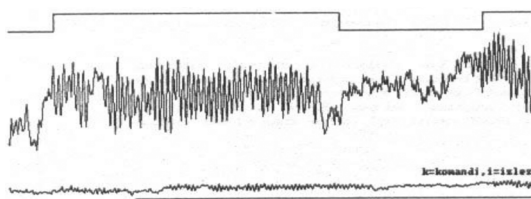


Fig. 3. Example of a mental switch and its EEG manifestation [18][19].

### III. MENTALLY EMULATED DIGITAL CIRCUITS

In this section, we will describe two mentally emulated control circuits: a mental action activated switch and a mental state flip-flop. The mental action switch changes a mental state and manifests it as a feature of an EEG signal, in this case an alpha rhythm amplitude change. The mental state flip-flop uses the CNV potential manifestation of an expectation mental state. If the CNV is present, it represents the Q state of the flip flop, and if the CNV is absent it represents the not-Q state of the mentally emulated flip-flop.

#### A. EEG Switch

An EEG switch is an EEG manifestation of a mental action in which a particular EEG feature changes in a way that it can be recognized by a computer. An example of an EEG switch is given in Fig. 3. It shows the EEG switch used in the 1988 BRI experiment [18], [19].

In the scenario of the corresponding 1988 experiment, the subject has a task to move a mobile robot from point A to point B along a trajectory drawn on the surface on which the robot is placed. While the subject's eyes are closed and the relaxation mental state is maintained, the mobile robot is moving along the trajectory. When the subject decides to exit the relaxation state and to look at the robot to see how far the robot is from the goal point, the EEG switch causes the robot to stop. Fig. 3 shows the screen of the 1988 brain-robot interface program [18], [19]. The lower part of the screen shows the complete EEG signal recorded in this particular session. Note that the section of the recorded EEG signal (bottom of the screen), which should be zoomed, is underlined. The zoomed section is shown in the central part of the screen. The upper part of the screen shows the effect of the mentally controlled EEG switch. The higher amplitudes of the EEG signal with dominant alpha rhythm in the middle of the screen show the mental state of relaxation in which

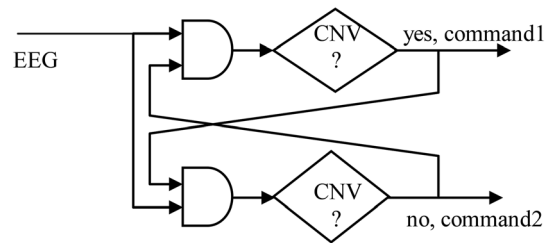


Fig. 4. CNV Flip-Flop.

the subject intentionally enters, usually by closing her/his eyes. The upper part of the screen shows the shaped output of the mentally controlled EEG switch. The computer software shapes the burst of the EEG alpha rhythm into a rectangle signal, emulating a switch of a Schmitt trigger type (e.g., [22]). The emulated Schmitt trigger output is sent to the robot to move when the brain is in the relaxed mental state and to stop when the brain is in the alert-and-focused mental state.

The mental action switch presented in Fig. 3 requires a period of training in order to perform the task. Some of the subjects engaged in the study were able to control the robot after 20 min of training. At the computational mental development part, a statistical machine learning method was used [19], [23] to learn to recognize the EEG switch and to produce a Schmitt trigger output.

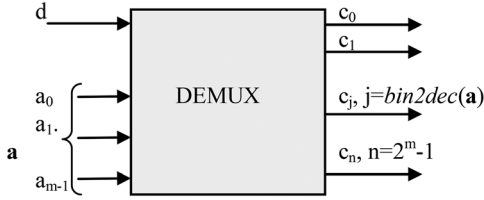
Let us note that the concept of a "mind switch" was introduced in [24]. Before that, the term "switching devices" [25] was used in relation to the independence of disabled persons. Here we introduce the term "mental switch," since we believe that this term is closely related to the study of mental development. The important point is that the switch is inside the brain; hence *it is a mental action*, while the manifestation of that action is in an emanated EEG signal, seen outside of the brain.

#### B. CNV Flip-Flop

A CNV flip-flop is an emulation of the flip-flop digital circuit based on the CNV evoked potential. The CNV potential [5] represents a mental state of expectation. Fig. 4 shows a mentally emulated CNV flip-flop.

In a CNV flip-flop design, an EEG signal is recorded in a CNV paradigm, in which manifestation of the expectation of a stimulus  $S_2$  after stimulus  $S_1$ ,  $\text{expect}(S_2|S_1)$ , is observed. When the CNV potential is recognized inside the recorded EEG, the  $S_2$  signal is blocked and a period of unlearning the expectation is taking place. As a result, the CNV potential will degrade beyond recognition, which will trigger the reactivation of the  $S_2$  signal. The flip-flop manifestation of the expectation mental state is observed. The digital output can be used to control external devices. The CNV flip-flop was used previously to control two robotic arms to solve the Towers of Hanoi problem with three disks [26].

Building a mentally emulated CNV flip-flop does not require separate subject training. The mental development of an expectation state is taking place in the course of the CNV experimental paradigm. In the CNV paradigm, the subject *learns to expect*. S/he learns that after event  $S_1$  comes event  $S_2$ , and s/he adjusts its mental state accordingly. The mental action produces a cognitive state "after  $S_1$  expect  $S_2$ ." At some point,

Fig. 5. Nonredundant 1-to- $2^m$  demultiplexer.

the mental state of expectation is developed to the extent where the CNV potential is recognizable as a feature of the observed EEG signal. At that point the program stops the stimulus S2. After some time of having no S2, the mental state of the subject changes towards the state of no-expectation. The mental action changes the mental state to “after S1 no expectation.” The mental state develops as a result of learning of the environment and its stimuli. The experimental paradigm often includes subject reaction to S2, so that a higher level of expectation prepares for a faster reaction.

Developing a pattern recognition program for the changing CNV potential requires a machine learning procedure. The CNV potential is a time varying event related potential and a standard averaging procedure to extract the signal is not applicable (e.g., [20]). So an adaptive filter is built which will track the time varying event related potential and recognize the point when that potential becomes a CNV potential, as well as when the CNV potential is not recognizable as such. As an output of the developed CNV flip-flop, the device is able to send the signal Q (expectation state present) and noQ (expectation state absent) in the subject mind.

#### IV. THE DEMULTIPLEXER AS A DIGITAL CIRCUIT

Digital circuits are nonlinear electric circuits and are often analyzed with compartmental approach [27]. In this section we will describe the demultiplexer as such a digital circuit. It is a communication and control structure which receives information through a single serial line and distributes it to one of the  $n$  parallel output lines, the selection of the output line being controlled by a set of separate input addressing lines. The demultiplexer paradigm has been traditionally used as an electronic circuit [22]. The realization of a demultiplexer can be either as a combinational circuit, or as a sequential circuit when it contains flip-flops. The simplest demultiplexer is the 1-to-2 demultiplexer. A special type of a demultiplexer is a redundant demultiplexer, used to improve the reliability and fault tolerance of systems [28][29]. The formal description of a demultiplexer can be given as follows:

A *demultiplexer* (or demux) is a circuit which receives serial data through a single line and distributes it to one of several parallel output lines. The outputs are gated, the gates being controlled by a bit-sequence of separate input addressing lines. A nonredundant demultiplexer has  $m$  addressing lines and  $2^m$  output lines. Fig. 5 shows the “black box” of a nonredundant demultiplexer.

As Fig. 5 shows, the demultiplexer has  $m$  addressing lines which define an address space of  $n = 2^m$  addresses, each addressing one of the  $n$  output lines. The data input  $d$  is sent to the addressed output line. Mathematically,

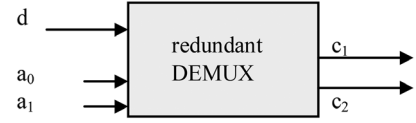


Fig. 6. A (1-to-2)(2) redundant demultiplexer.

$\text{val}(c_j) = d$  where  $j = \text{bin2dec}(\mathbf{a})$  where  $\text{val}(c_j)$ ,  $j \in \{0, 1, \dots, 2^m - 1\}$  is the value of the selected  $j$ -th output line,  $j$  is the decimal order number of the selected output line,  $\text{bin2dec}(\ )$  is a binary-to-decimal *decoder* function,  $\mathbf{a} = a_{m-1}, a_{m-2}, \dots, a_1, a_0$  is the  $m$ -line input addressing bus, and  $d$  is the input value. The mapping  $\text{bin2dec}(\ )$  is nonredundant, in a sense that  $m = \log_2 n$ , and the map is bijective, i.e., each binary address corresponds to one and only one output line.

A more relaxed specification is given by the following definition: A demultiplexer is a serial-to-parallel converter which has one data input, several addressing inputs, and several outputs. The output to which the data input will be transferred is selected by the bit combination of the addressing inputs.

This definition suggests a design choice of having a redundant addressing scheme with  $m$  addressing lines and less than  $2^m$  output lines. This enables having a redundant address encoding for error tolerance and improved reliability. As an example, consider a 1-to-2 demultiplexer: it needs only one addressing line for encoding the two output lines. However, for error tolerance, two addressing lines can be used. Instead of encodings “0” and “1” for two outputs, the encodings “01” and “10” can be used, which adds to error tolerance by increasing the Hamming distance. In the case that the error codes “00” and “11” occur, a classification might be added, named “no operation”, so that no output would be addressed.

A *redundant demultiplexer* can be mathematically described as

$$\text{val}(c_j) = d, \quad d \in R$$

$$j \in \{1, 2, \dots, n\}, n \leq 2^m,$$

$$j = g(a_{m-1}, a_{m-2}, \dots, a_1, a_0), a_k \in \{0, 1\}, k \in \{0, 1, \dots, m-1\}$$

where  $\text{val}(c_j)$  is the value of the selected output  $c_j$ ,  $j \in \{1, 2, \dots, n\}$  is the decimal order number of the selected output line,  $\mathbf{a} = a_{m-1}, a_{m-2}, \dots, a_1, a_0$  is the  $m$ -line demultiplexer addressing bus,  $d$  is the input data which in general can be a real number, and  $g(\ )$  is the mapping between the input and the output lines.

In a redundant demultiplexer, the relation between the number of addressing lines  $m$  and the number of output lines  $n$  is  $m \geq \log_2 n$ . The mapping  $g(\ )$  is redundant, in a sense that it is possible that more than one addressing combinations encode the same output line. The mapping can also be partial, such that there are bit-combinations that do not address an output line. Thus, the standard notation “1-to- $n$ ” (or 1:n) is not sufficient to describe a redundant demultiplexer. The notation (1-to- $n$ )( $m$ ) is used in this paper to specify that in a considered redundant demultiplexer there are  $n$  output lines and  $m$  address lines (satisfying  $m \geq \log_2 n$ ). An instance is the (1-to-2)(2) redundant demultiplexer, shown in Fig. 6.

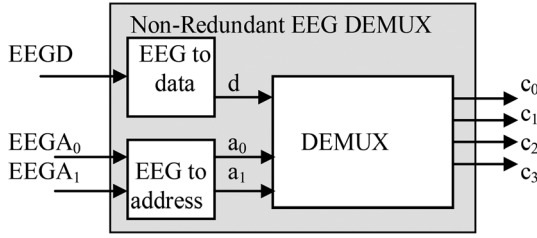


Fig. 7. A 1-to-4 nonredundant EEG demultiplexer.

As Fig. 6 shows, a redundant (1-to-2)(2) demultiplexer uses two addressing lines. In a nonredundant design, the address line  $a_0$  would be enough to address the two outputs  $c_1$  and  $c_2$ , for example by encoding  $a_0 = 0$  for  $c_1$  and  $a_0 = 1$  for  $c_2$ . However, if for some reason it is assumed that  $a_0 = 0$  is not a reliable input, a redundant address line  $a_1$  is then added. The new, redundant, addressing bus is  $a_1a_0$  and the output channels can be addressed with  $a_1a_0 = 01$  for  $c_1$  and  $a_1a_0 = 1X$  for  $c_2$ , where  $X$  is either binary 0 or 1. So, *by redundant design*, the influence of the nonreliable input  $a_0 = 0$  is avoided.

In addition to the principal demultiplexer components such as the binary-to-decimal address decoder and the output gates, flip-flops can be added to the demultiplexer design to be used as latches. One example of using a demultiplexer with latched addresses is when the demultiplexer transmits signals (analog or binary) of various durations. The output gates should be kept open throughout the transmission of such data. A stream of digital data can also be transmitted by a latched demultiplexer. The output address is latched, the data stream is sent while the address remains unchanged, and, when needed, a new address is latched and another stream of data of a possibly different length is sent through a different demultiplexer output.

## V. MENTALLY EMULATED EEG DEMULTIPLEXER

Here we will describe a mentally emulated EEG demultiplexer, or in short an EEG demultiplexer.

An EEG demultiplexer contains two internal EEG decoders: 1) the *EEG-to-address* decoder and 2) the *EEG-to-data* decoder. Information is encoded in an EEG signal by a subject who generates that signal. An instance of a nonredundant EEG demultiplexer is shown in Fig. 7.

Mathematically, an EEG demultiplexer can be represented as a pair of equations. A formal description of the EEG demultiplexer concept can be stated as:

An *EEG demultiplexer* is a system with a data input  $D$  and addressing inputs  $A_{m-1}, A_{m-2}, \dots, A_1, A_0$ , all of which are EEG signals. The EEG signals  $EEGA_{m-1}, EEGA_{m-2}, \dots, EEGA_1, EEGA_0$ , received through the addressing inputs, encode a binary address  $a_{m-1}a_{m-2} \dots a_1a_0$ , which addresses one of the  $n$  demultiplexer outputs  $c_j$  ( $j = 1, 2, \dots, n$ ). The EEG signal  $EEGD$ , received through the data input, in general encodes real valued data  $d$ . Once one of the outputs  $c_j$  is selected, the data  $d$  are sent to that output. It holds true that  $n \leq 2^m$ , where  $n$  is the number of outputs, which allows for a redundant design.

The binary address  $a_{m-1}a_{m-2} \dots a_1a_0$  is obtained from the signals  $EEGA_{m-1}, EEGA_{m-2}, \dots, EEGA_1, EEGA_0$  by a function named *EEG-to-address decoder*, and the data

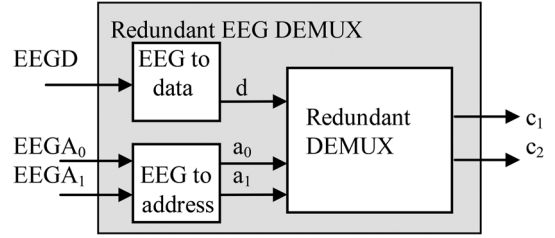


Fig. 8. A (1-to-2)(2) redundant EEG demultiplexer.

$d$  are obtained from the signal  $EEGD$  by a function named *EEG-to-data decoder*. They are defined as

$$a_k = p(\text{feature}(EEGA_k)), k = 0, 1, \dots, m - 1 \quad (1)$$

$$d = h(\text{feature}(EEGD)). \quad (2)$$

Equation (1) represents the EEG-to-address decoder:

- $k = 0, 1, \dots, m - 1$  is the index of the demultiplexer addressing lines;
- $EEGA_k$  is the EEG signal on the  $k$ -th address line;
- $\text{feature}(\ )$  is the feature-signal extracted from the EEG signal;
- $p(\ )$  is a binary decision function, deciding whether the obtained  $\text{feature}(EEGA_k)$  signal is salient, i.e., above some threshold value;
- $a_k$  is the binary valued, decoded addressing line.

Equation (2) represents the EEG-to-data decoder:

- $EEGD$  is the EEG signal with encoded data input  $d$ ;
- $h(\ )$  is a function that decodes the data  $d$  from the  $\text{feature}(EEGD)$  signal.

In a narrative description, the EEG-to-address decoder decodes the mentally generated EEG signal into a binary pair  $(a_0, a_1)$ . Binary “1” means that a mental switch has activated an EEG feature of interest (e.g., alpha rhythm), while binary “0” means that the EEG feature is absent. The EEG-to-data decoder decodes a particular region of the mentally generated EEG signal into a real valued data. An instance of the above defined EEG demultiplexer is the (1-to-2)(2) EEG redundant demultiplexer, shown in Fig. 8.

One of the two addressing lines in Fig. 8. is redundant. The redundancy is added due to the nature of the input EEG signals: they are intentionally generated by a mental action of a subject, and it is expected that the subject’s intent will not always be reliably manifested as a particular EEG segment.

## VI. REALIZATION OF AN EEG DEMULTIPLEXER

In an EEG demultiplexer realization, the addressing inputs  $EEGA_{m-1}, EEGA_{m-2}, \dots, EEGA_1, EEGA_0$  can be obtained either from  $m$  different EEG channels, or from less than  $m$  different channels, meaning that one EEG channel would encode more than one address. The challenge in the realization described here is to design an EEG demultiplexer which has only one EEG channel for encoding both the addressing lines and the data line.

Since there is only one channel, the information can be encoded in segments (frames) of the EEG signal. Let the EEG signal be divided into  $m$  EEG *frames*,  $A_{m-1}, A_{m-2}, \dots, A_1, A_0$ . Each frame  $A_k$  contains an EEG *signal segment*  $EEGA_k(t)$  ( $k = 0, 1, \dots, m - 1$ ) that encodes a

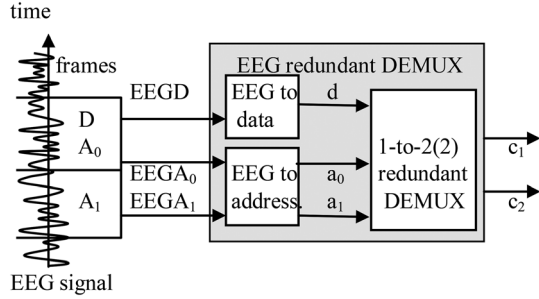


Fig. 9. EEG frames providing inputs to a (1-to-2)(2) EEG redundant demultiplexer.

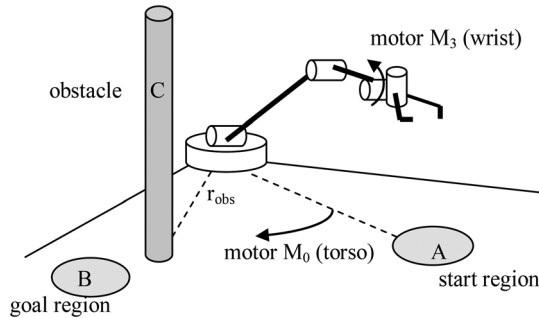


Fig. 10. Proof-of-the-concept demonstration. Using EEG control, a subject should utilize a mentally emulated (1-to-2)(2) EEG redundant demultiplexer to control two motors of a robot arm to move the arm from a start region A towards a goal region B avoiding an obstacle C along the way.

subject generated information. Such a sequence of EEG signal segments received through a single EEG channel here is called an *EEG sentence*.

Fig. 9 shows an EEG demultiplexer with an EEG sentence encoded in two frames. In this realization, both the address  $a_0$  and the data  $d$  are decoded from the same EEG frame. Address  $a_0$  will be binary valued, and data  $d$  will be integer valued.

In each EEG frame the subject tends to generate an EEG feature (e.g., increased amplitude of the alpha rhythm) that will be interpreted by both the EEG-to-address and the EEG-to-data decoders.

## VII. DEMONSTRATION SCENARIO FOR THE PROOF OF THE CONCEPT

To give a proof of the EEG demultiplexer concept, a demonstration scenario is designed as shown in Fig. 10. The subject observes a scene in which a robotic arm should move from a start region A to a goal region B, while avoiding an obstacle C along the way.

The scenario uses a 5-motor robotic arm in which only two motors are allowed to move (i.e., two degrees of freedom are allowed), while the other three motors are fixed in some predefined positions. The controlled motors are motor  $M_0$  (torso) for azimuth (horizontal) movement, and motor  $M_3$  (wrist) for elevation (vertical) movement. The robot arm moves horizontally, and at the point in which the robotic arm reaches the obstacle, its horizontal projection should be less than  $r_{obs}$ , where  $r_{obs}$  is the horizontal distance between the robot arm base and the obstacle. The movement of  $M_3$  (wrist) can shorten the horizontal projection of the arm, so that the arm would avoid the obstacle.

Let  $\varphi(M_j)$ ,  $j \in \{0, 3\}$  be a function of a motor position (rotation angle). The robot used in this demonstration is a product of Lynxmotion, with Hitec motors controlled by a SSC-32 Servo Controller [30] which accepts positions as positive integer values, ranging from 0 to 255. The initial position of a motor is 127 and when  $\varphi(M_0) = \varphi(M_3) = 127$  it is said that the robot arm is in its initial (default) position. The geometry of the demonstration scenario is such that the movement of the robot arm towards the goal region decreases the values of  $\varphi(M_0)$ , while the movement of the robot wrist upwards increases the values of  $\varphi(M_3)$ . The obstacle is placed at position  $\varphi(M_0) = 35$ . The obstacle can be avoided if  $M_3$  has the elevation of minimum  $\varphi(M_3) = 220$  when  $M_0$  is approaching and passing the obstacle. Mathematically, the goal region of the robot arm internal coordinate space ( $\varphi(M_0)$ ,  $\varphi(M_3)$ ) is the region

$$35 \geq \varphi(M_0) \geq 0 \quad \text{and} \quad 220 \leq \varphi(M_3) \leq 255. \quad (3)$$

The task for the subject is to take series of mental actions and generate a series of EEG signals that will move both  $M_0$  from its default start position A to a goal position B, and  $M_3$  from its default start position to a vertical position which has enough elevation to avoid an obstacle C along the way of  $M_0$ . The subject, who executes the needed mental actions to control the movement of the robotic arm, does not know the digital values of the motors. S/he visually observes the scene and tries to execute mental actions to generate EEG signals to move a robot arm according to her/his planned trajectory.

## VIII. METHODS

This section describes the application setup and elaborates the elements of the setup.

### A. Application Setup

The application setup is given in Fig. 11. In this setup, the timer has a period of  $T = 7 + 12$  s. The first 7 s (trial time) are for the subject's intent encoding in EEG and the EEG acquisition, and the next 12 s (inter-trial interval) are for robot movement as well as for the subject's observation and planning of the next mental command. Such a timer allows the subject to generate up to three EEG encoded commands per minute ( $60s/T = 3$ ) for controlling the EEG demultiplexer and the robot arm connected to it. The sampling frequency is 100 Hz, so 700 samples of the acquired EEG signal are analyzed in each trial.

### B. Elements of the Application Setup

The application setup consists of: 1) the subject; 2) EEG acquisition; 3) EEG signal conditioning; 4) features extraction; 5) pattern recognition and decision making; 6) demultiplexer: EEG to data decoder; 7) demultiplexer: latched design and the output; and 8) interface to the motors and demonstration scenario.

### C. Human Subject

The human subject observes the demonstration scenario and performs mental actions generating EEG inputs to a mentally emulated EEG demultiplexer, which controls the movement of the robotic arm. The subject plans which robot arm motor should be moved next. Then s/he tries to enter into a mental state of

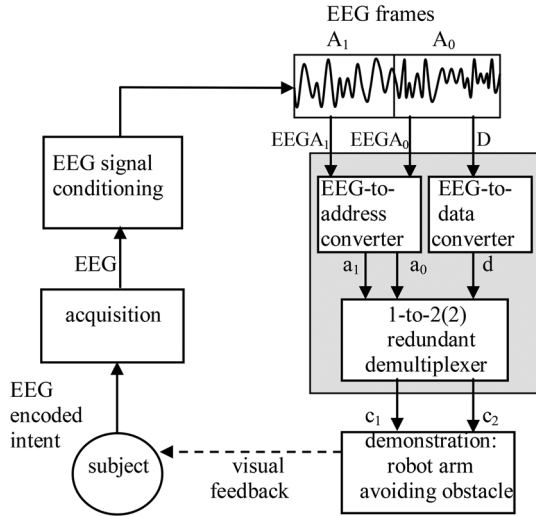


Fig. 11. EEG demultiplexer: Application setup.

relaxation at some particular time of the experimental trial in order to generate an EEG signal that would execute the planned movement.

#### D. EEG Acquisition

The international 10–20 system [31] is used for determination of the spatial distribution of electrodes on the subject’s scalp. The electrode placement defines the brain regions of interest. The number of electrodes for recording alpha rhythm recording is between 1 and 8 [32]. In this experimental investigation, a single channel is used with two electrodes placed at P3 and PO7 points of the 10–20 international system, with the ground electrode placed at the left mastoid.

#### E. EEG Signal Conditioning

A low-pass filter of 0–30 Hz is used to eliminate artifacts that are outside the EEG spectrum of interest. Such a filtered signal will be shown on the screen. In addition, an alpha rhythm (8–13 Hz) band pass filter is used, which eliminates the artifacts out of that frequency range, which will also be shown on the screen. From the acquired EEG signal, only the alpha rhythm is extracted for further processing.

Afterwards, such a processed EEG signal is divided into EEG frames. The signal is received in 700 samples from the 7-s EEG acquisition window. One second from each end of the acquired signal is deemed unfit for further processing, so that artifacts that arise due to signal cut-off at the start and the end of acquisition would not be taken into account. The remaining middle 5 s are divided into two EEG frames, each 2.5 s wide. The frames are denoted by  $A_1$  and  $A_0$ , respectively. Each of the two frames contains 250 EEG samples. Mathematically, the EEG signals inside the frames can be described as

$$EEGA_k(t) \quad k \in \{0, 1\}; t \in \{1, 2, \dots, 250\}. \quad (4)$$

#### F. Feature Extraction Method

The EEG feature of interest is the command given by the subject encoded in the intensity of the alpha rhythm. Our approach is to view the entire process as an *EEG modem*. Using this view,

the command is *modulated* by the EEG signal and is *demodulated* from it. The EEG is viewed as a carrier signal, the alpha rhythm as modulated (message) signal, and the intensity of the alpha rhythm as encoded intended command. So our view is a view of an Amplitude Modulation (AM) and demodulation process. A method of demodulation of an AM signal in electronics is to use of a full-wave rectifier and then use a low-pass filter (e.g., [33]). The low-pass filter actually approximates the envelope of the demodulated signal, and is a measurement of its intensity.

After the extraction of the alpha band (8-13 Hz) from the signal  $EEGA_k$ , a new signal named  $\text{Alpha}A_k(t)$  is obtained

$$\begin{aligned} \text{alpha}A_k(t) &= \alpha(EEGA_k(t)) \\ k(0, 1; t \in \{1, 2, \dots, 250\}) \end{aligned} \quad (5)$$

where the function  $\alpha()$  is 8-13 Hz band-pass filtering. The band-pass filter 8-13 Hz also eliminates artifacts outside the filtered band. In AM terminology, this is our modulated signal. For demodulation, the absolute value of that signal is computed, which is actually the function of a full-wave rectifier. The envelope of that signal can now be extracted by a low pass filter, which has a cut-off frequency below the frequency of the modulated signal [34], which in our case is below 8 Hz, the lower border frequency of the alpha band.

We have chosen to use low pass filter 0-3 Hz filter because it is the frequency of the EEG  $\delta$ -rhythm which is below a frequency of other EEG rhythms. The obtained signal after this low pass filter can be viewed as a new EEG rhythm which we name the alpha-delta rhythm.

Let  $\delta()$  represent the lowpass filter 0-3 Hz, and let  $\text{abs}()$  be the absolute value function. The feature extraction function is thus defined as

$$\begin{aligned} \text{feature}A_k(t) &= \delta(\text{abs}(\alpha(EEGA_k(t)))) \\ k \in \{0, 1\}; t \in \{1, 2, \dots, 250\}. \end{aligned} \quad (6)$$

The equation (6) is an elaboration on the equation (1). It presents a method of computing the intensity of the alpha rhythm. The intensity here is a demodulated message carried out as amplitude modulation (AM) of the alpha band carrier signal.

Let us note that we use the amplitude of the alpha rhythm because it enables hard real time applications. In a hard real time application an action can be sent to the robot between any two samples of the EEG signal. However, because of the possibility of artifacts, usually several amplitudes are counted before a decision is made whether an amplitude has a particular value because of the event observed or it is just an artifact [18]–[23].

#### G. Pattern Recognition Method

The pattern recognition method computes the binary decision of whether the extracted feature is salient enough in an EEG frame. The binary decision is computed by introducing a count variable  $C_k$ , which counts how many times the amplitude of the  $\text{feature}A_k(t)$  signal is greater than a predefined *amplitude threshold*  $\theta_a$ ; if the count variable  $C_k$  is larger than a predefined *count threshold*  $\theta_c$ , then the  $\text{feature}A_k(t)$  is declared present in the observed EEG frame  $k$ . Both the amplitude threshold  $\theta_a$  and the count threshold  $\theta_c$  are parameters of the pattern recognition method, and are determined specifically to the application. The

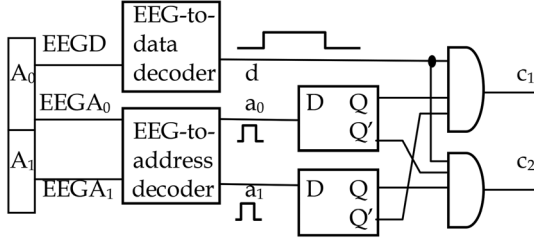


Fig. 12. Latched design of the (1-to-2)(2) EEG demultiplexer, performing operations if( $a_1a_0 = 01$ ) $c_1 = d$ ; if( $a_1a_0 = 10$ ) $c_2 = d$ .

values that we use in our application are reported in the application section later in this paper. Mathematically, the decision is made using the equations

$$C_k = \sum_{t=1}^{250} \text{sgn}(\text{feature}A_k(t) - \theta_a); k \in \{0, 1\} \quad (7)$$

$$a_k = \text{sgn}(C_k - \theta_c), k \in \{0, 1\} \quad (8)$$

where  $\text{sgn}()$  is a function which gives “1” for a nonnegative argument and “0” for a negative argument.

The values obtained by the  $\text{sgn}()$  function are interpreted as binary decision values. The ordered pair  $a_1a_0$  of binary values defines the binary address of an output gate of the (1-to-2)(2) EEG demultiplexer.

#### H. Demultiplexer: EEG-to-Data Decoder

The EEG demultiplexer data line is obtained from the EEG data frame  $D$ , which is also the address frame  $A_0$ . Once the integer value of  $C_0$  is obtained using (7), the integer value of the data line is computed as

$$d = C_0 \text{sgn}(C_0 - \theta_c). \quad (9)$$

In other words,  $d = C_0$  if the count  $C_0$  is greater than the count threshold  $\theta_c$ , otherwise  $d = 0$ .

#### I. Demultiplexer: Latched Design and the Output.

The data value  $d$  obtained by (9) is represented as the duration of the output binary signal. This requires a latched design of the EEG demultiplexer, to allow binary signals of various durations to be carried out through an output gate while the gate is kept open by the latch. Since the addressing bus has two lines ( $a_1a_0$ ), two address latches are needed. An example of a realization of a latched redundant demultiplexer is shown in Fig. 12.

The latched design shown in Fig. 12 allows a binary signal of a variable duration to pass through one of the two output gates. The notation  $Q'$  is used for the binary complement of the flip-flop state  $Q$ .

The latched design allows the operation mode in which first the address is latched and then a signal of variable length is sent without an address change.

The EEG demultiplexer is controlled by a subject who is able to produce an EEG signal in the frames pair  $A_1A_0$ , so that the signal will be decoded into a binary address  $a_1a_0$ . It is realized that the subject will have difficulties generating the EEG signal that will be decoded into  $a_1a_0 = 10$ . This would require the subject to generate the alpha rhythm only in the  $A_1$  frame of 2.5 s. To avoid the need of generation of the address  $a_1a_0 =$

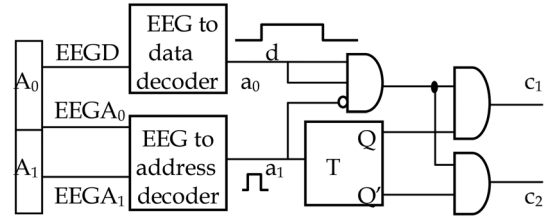


Fig. 13. Design for a (1-to-2)(2) EEG demultiplexer. The two D-latches are replaced by one T flip-flop. The operations performed are: if( $a_1a_0 = 01$ ) $\text{val}(c_j) = d$ ; if( $a_1a_0 = 1X$ ) change  $j$ ;  $j \in \{1, 2\}$ .

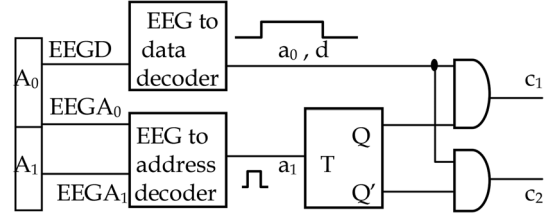


Fig. 14. Optimized design for the (1-to-2)(2) EEG demultiplexer. The operations performed are: if( $a_1a_0 = 0X$ )  $\text{val}(c_j) = d$ ; if( $a_1a_0 = 1X$ ) change  $j$ ;  $j \in \{1, 2\}$ .

10, the following design of the redundant EEG demultiplexer is implemented

$$\text{if } a_1a_0 = 01 \text{ then } \text{val}(c_j) = d, j \in \{1, 2\} \quad (10.1)$$

$$\text{if } a_1a_0 = 1X \text{ then change } j, j \in \{1, 2\} \quad (10.2)$$

$$\text{if } a_1a_0 = 00 \text{ then no operation.} \quad (10.3)$$

With the redundant design given in equations (10), in order to change the EEG demultiplexer address, the subject can generate alpha rhythm starting in frame  $A_1$  and lasting longer than duration of frame  $A_1$  ( $a_1a_0 = 1X$ ), which is easier and more reliable than to generate alpha rhythm only in a rather narrow frame  $A_1$  of 2.5 s ( $a_1a_0 = 10$ ).

The design of the redundant demultiplexer according to (10) is shown in Fig. 13.

The design uses a single memory element (T flip-flop) rather than using two memory elements (D flip-flops). Further optimization of the redundant design (10) can be obtained by assuming the “no operation” condition  $a_1a_0 = 00$  is a situation in which the output  $d$  is produced with value  $d=0$ . This enables the following design:

$$\text{if } a_1a_0 = 0X \text{ then } \text{val}(c_j) = d, j \in \{1, 2\} \quad (11.1)$$

$$\text{if } a_1a_0 = 1X \text{ then change } j, j \in \{1, 2\} \quad (11.2)$$

which is shown in Fig. 14.

The optimized redundant design in Fig. 14 uses the data line  $d$  as address line  $a_0$ . This is possible since both variables are computed from the same EEG frame  $A_0$ . If  $a_0 = 1$  then the data line generates a binary signal of duration  $d$ , and if  $a_0 = 0$  then the data line generates a signal with duration  $d = 0$ , meaning no signal.

#### J. Interface to Motors and the Demonstration Scenario

The demonstration uses the scenario described previously in Fig. 6. In the scenario, the subject is able to generate the EEG signals  $EEGA_1$  and  $EEGA_0$ , which will control the output lines



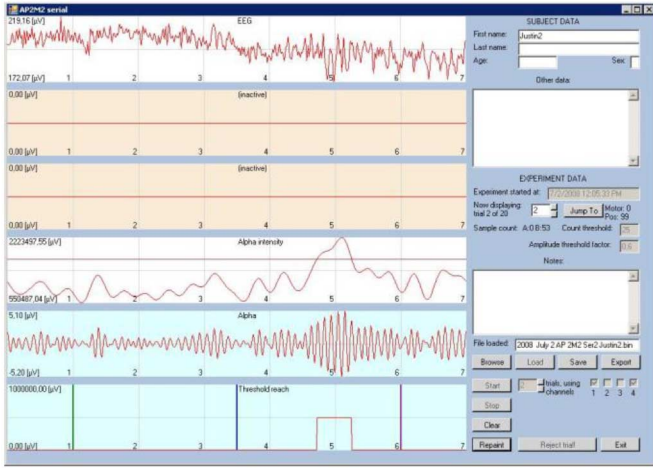


Fig. 15. The screen of the implemented software.

$c_1$  and  $c_2$  of the EEG demultiplexer, which in turn will control the motors  $M_0$  and  $M_3$  of the robotic arm.

The interface between the demultiplexer outputs  $c_j$ ,  $j \in \{1, 2\}$  and the motors  $M_i$ ,  $i \in \{0, 3\}$  is defined by

$$i = j + (-1)^j \quad (12)$$

which in other words means that

$$\begin{aligned} \text{if } j = 1 & \text{ then } i = 0 \\ \text{if } j = 2 & \text{ then } i = 3 \end{aligned}$$

Once the motor index  $i \in \{0, 3\}$  is determined, the signal transmitted through the demultiplexer output will move the motor proportionally to the data  $d$

$$\varphi(M_i) = h(d), i \in \{0, 3\} \quad (13)$$

where  $h()$  is an integer valued function of an integer argument. The data  $d$  is obtained in the aforementioned equation (9).

## IX. IMPLEMENTATION SOFTWARE

This section of the paper describes the software that implements the presented EEG demultiplexer. The software is written in the C# programming language. Fig. 15 shows the screen for carrying out the proof-of-the-concept experiments.

The screen is organized in two sections: a right-hand side one and a left-hand side one. The right-hand side section contains information about the experiment. Besides the information about the subject and about the log file of the experiment, this part of the screen shows two experiment parameters: the amplitude threshold  $\theta_a$  and the count threshold  $\theta_c$ , which are kept constant throughout the experiment. Those parameters are chosen by the user of this EEG Demultiplexer software for a particular application. The left-hand side section is the EEG demultiplexer computation section. It is divided into six display channels for acquired or computed waveforms, four of which are used in this experimental investigation. Those four channels show the EEG signal obtained and how it is processed. The two channels not used in this presentation are sometimes used for EOG and EMG channels to observe artifacts.

The duration of the display channels in this investigation is 7 s. The first display channel shows the acquired and preprocessed EEG signal, generated intentionally by the subject. The fifth display channel shows the extracted alpha rhythm from the EEG signal shown in display channel 1, according to the equation (5). The fourth display channel shows the extracted feature waveform, i.e., the alpha-delta rhythm computed as  $\delta(\text{abs}(\alpha(\text{EEG})))$  as shown in equation (6), while  $\alpha(\text{EEG})$  is shown in channel 5. Thus, the fourth channel represents a measure of intensity of the alpha rhythm. It also shows the amplitude threshold  $\theta_a$ , (horizontal line). The amplitude values above the threshold contribute towards a decision whether the observed alpha rhythm is salient enough. The sixth display channel shows the final step of the EEG demultiplexer computation. It shows the segmentation (vertical bars) of the 7-s acquisition window. The middle 5 s are divided into two 2.5-s frames: The left side frame is  $A_1$  and the right side one is  $A_0$ . The right side frame  $A_0$  is also the data frame  $D$ .

In the particular trial shown in Fig. 15, it can be seen that:

- 1) In frame  $A_1$  (left-hand side frame) there was no salient alpha rhythm. All alpha rhythm activity is below the amplitude threshold; thus the demultiplexer address will be  $a_1 = 0$ .
- 2) In frame  $A_0$  (right-hand side frame) there is the appearance of a  $\text{sgn}()$  signal. This means that the salient alpha rhythm was recognized (amplitude of the intensity of the alpha rhythm was above the amplitude threshold -- see display channel 4) in a number of samples  $C_k$ , which was greater than the count threshold  $\theta_c = 25$  set in the right-hand side section of the screen (Fig. 15). This, in turn, determines that the demultiplexer addressing line  $a_0$  has the value  $a_0 = 1$ .

So, in Fig. 15, the address is computed as  $a_1 a_0 = 01$ , according to (8). The data value  $d$  is computed according to (9), and is shown as the duration of the  $\text{sgn}()$  function in frame  $A_0$ . Accordingly, a motor will be moved proportionally to the width of the  $\text{sgn}()$  function shown in frame  $A_0$ .

## X. EXPERIMENTAL INVESTIGATION

The experimental investigation setup is shown in Fig. 16. A separate room is designed for the experiments, with a glass door, through which the photo shown in Fig. 16 is taken.

The human subject sits in front of an industrial 19" rack on which the computer, the robotic arm, and the biopotential amplifier (top of Fig. 16) are placed. A white vertical rod is placed on the trajectory of the arm moving counter-clockwise. The EEG signal is recorded by bipolar measurement, between electrodes placed at P3 and PO7 with the ground electrode on the left mastoid. The electrodes and a 4-channel biopotential amplifier (MP35) we use are products of Biopac [35]. In the case of much hair present (as in the case shown in Fig. 16), we use EL120 electrodes, and in the case of not much hair present we use EL503 electrodes. The amplifier is connected to a Windows-based personal computer via a USB port.

The computer communicates with a microcontroller-based servo-controller (SSC32), which is built into the robot platform. The servo controller receives commands from the computer and performs smooth and parallel movement of the robot arm's digital servo motors.



Fig. 16. Experimental lab setup.

The subject has visual feedback of the effect of her/his EEG commands. The start and the end of the 7 s EEG acquisition (trial time) are indicated by an external clue, namely a beep sound. The two frames inside the acquisition window are not separated by an external clue -- the subject herself/himself estimates the frame s/he is in, and decides when to increase or decrease the intensity of the EEG alpha rhythm. During the 12 s intertrial interval the subject observes the scene and plans the next EEG intent. In this period the subject can blink and otherwise make the work more comfortable.

The subject is instructed that:

- 1) In order to generate salient alpha rhythm in a particular EEG frame, s/he should enter a relaxation state and have her/his eyes closed in that frame;
- 2) To change the addressed motor the subject should enter the relaxation state immediately after the acquisition start beep inside frame  $A_1$ . S/he can close the eyes even before frame  $A_1$ , and can keep them closed for a prolonged time, which is allowed by the error tolerant, redundant design ( $a_1a_0 = 1X$ ) of the EEG-to-address decoder. The eyes can remain closed even after the stop beep is heard;
- 3) In order to move a motor, the subject should pay attention not to enter the relaxation state for 3 s after the start beep, while her/his EEG is in frame  $A_1$ . To avoid the generation of alpha rhythm, a possible strategy is to count silently “21, 22, 23” or perform some other mental action which would block a salient alpha rhythm. Afterwards, while in frame  $A_0$ , the subject should try to enter relaxation state before the end-of-acquisition beep.

The initial conditions for each experiment in this experimental investigation are:

- The latched design defines  $c_1$  as the default output line,
- The amplitude threshold parameter is set to 0.6 (right-hand side on Fig. 15), which means that the amplitude threshold line is set at 60% of the peak-to-peak range of the alpha rhythm intensity waveform. Mathematically,  $\theta_a = 0.6(\text{feature}A_k(t))_{p-p}$ ,
- The count threshold is set to  $\theta_c = 25$  (right-hand side on Fig. 15), which means that the alpha rhythm intensity should be above the amplitude threshold  $\theta_a$  in at least 25 samples, in order for the alpha rhythm in that particular

TABLE I  
EXAMPLE OF AN EXPERIMENT LOG

Trial	EEG Demultiplexer					Robot		
	Threshold $\theta_c=25$				Out- put line	Motors		
	$a_k = \text{sgn}(C_k - \theta_c)$					motor	com- mand	posi- tion
	$C_1$	$a_1$	$C_0$	$a_0$				
1	20	0	0	0	$c_1$	$M_0$	NoOP	127
2	23	0	36	1	$c_1$	$M_0$	Move	112
3	1	0	88	1	$c_1$	$M_0$	Move	89
4	5	0	45	1	$c_1$	$M_0$	Move	76
5	0	0	62	1	$c_1$	$M_0$	Move	60
6	0	0	28	1	$c_1$	$M_0$	Move	53
7	23	0	31	1	$c_1$	$M_0$	Move	39
8	77	1	4	0	$c_2$	$M_3$	Switch	127
9	11	0	43	1	$c_2$	$M_3$	Move	138
10	0	0	47	1	$c_2$	$M_3$	Move	150
11	0	0	35	1	$c_2$	$M_3$	Move	159
12	0	0	44	1	$c_2$	$M_3$	Move	170
13	2	0	55	1	$c_2$	$M_3$	Move	184
14	0	0	75	1	$c_2$	$M_3$	Move	203
15	0	0	65	1	$c_2$	$M_3$	Move	220
16	0	0	65	1	$c_2$	$M_3$	Move	237
17	25	1	17	0	$c_1$	$M_0$	Switch	39
18	0	0	19	0	$c_1$	$M_0$	NoOP	39
19	0	0	54	1	$c_1$	$M_0$	Move	25

frame to be recognized as salient (Fig. 15., display channel 6).

#### XI. RESULTS, PROOF OF THE CONCEPT, AND BEYOND

For each experiment, the implementation software generates an experiment log file. Table I shows a log of an experiment.

The first column of Table I is the order number of an experiment trial. This particular experiment lasted for 19 trials before its successful completion. Column 2 and column 3 show the EEG-to-address decoder function for frame  $A_1$ . Analogously, column 4 and column 5 show the EEG-to-address decoder for frame  $A_0$ . Column 6 shows the addressed output line ( $c_1$  or  $c_2$ ) of the EEG demultiplexer. Column 7 shows the motor ( $M_0$  or  $M_3$ ) addressed by the output line of the demultiplexer. Column 8 shows the command (Move, Switch, and NoOperation) the motor is receiving in that trial. Column 9 shows the positions of the motors after the execution of the command in each trial, and consequently this column shows the robot arm trajectory throughout the experiment.

To follow a numeric example, consider trial 2. Column 2 shows the count value  $C_1 = 23$ , which is below the count threshold  $\theta_c = 25$  and consequently the computation  $a_1 = \text{sgn}(C_1 - \theta_c)$  gives 0 in column 3. Analogously, for columns 4 and 5 in trial 2: since  $C_0 = 36$ , the address line  $a_0 = 1$ . Column 6 has the value  $c_1$ , since the redundant address  $a_1a_0 = 01$  does not change the default address  $c_1$ . Column 7 shows that the addressed motor is  $m_0$ . Column 8 shows that the motor moves. Column 9 shows that the motor  $M_0$  moved from its initial position  $\varphi(M_0) = 127$  to a new position  $\varphi(M_0) = 112$ .

Note that in both trial 17 and 18, the motors did not move, and that it is due to two different reasons. In trial 17, an address change took place and the latched EEG demultiplexer changed the motor address but did not move it. In trial 18, the subject was not able to generate a salient alpha rhythm in either frame: both count values  $C_1 = 0$  and  $C_0 = 18$  were below the threshold

$\theta_c = 25$ , so neither a new address nor new data were generated. There are two more cases in Table I where motors did not move: in trial 1, there was no salient alpha rhythm and in trial 8 there was an address change.

A successfully completed task requires that the obstacle avoidance criterion given by equation (3) be satisfied. In the considered experiment, the task was successfully completed: in trial 18 motor  $M_0$  moved from  $\varphi(M_0) = 39$  to  $\varphi(M_0) = 25$ , passing the obstacle at  $\varphi(M_0) = 35$ , while motor  $M_3$  had elevation of  $\varphi(M_3) = 237$  achieved before trial 18, namely in trial 16.

#### A. Representation of the Results in an Achievement Motivation Space

The task used as proof of the concept can be viewed as a task of generating a robot trajectory from a start state to a goal (achievement) state, avoiding unpleasant states. Such a task can be described in terms of achievement motivation space. A set of states can be observed in some state space which has emotionally colored states where the goal states are marked with a positive emoticon (usually ☺) whereas states to be avoided are denoted with a negative emoticon (usually ☹). The achievement motivation concept has been around in psychology since the 1950-es [36][37]. Emoticons have been used previously in representing state spaces with emotionally colored states (e.g., [38]).

For the coordinates of the achievement motivation space of the subject, we use the internal coordinates of the robot arm, i.e., the position of its motors. Using direct kinematics, they can be represented as external space coordinates. For that reason our achievement motivation space is defined as a two-dimensional ( $\varphi(M_0)$ ,  $\varphi(M_3)$ ) space, where each coordinate is a position (rotation) of a corresponding motor. The space is shown in Fig. 17. The trajectory of the robot arm movement shown is obtained from the experiment data given in Table I.

In the experiment represented in Fig. 17, the subject, using an EEG demultiplexer, chose to control the motor  $M_0$  first. The subject used 6 mental actions and moved the robot near the obstacle at the azimuth  $\varphi(M_0) = 35$ . Then the subject switched the EEG demultiplexer output to motor  $M_3$ . Then the subject with 8 mental actions moved the robot beyond the needed elevation of  $\varphi(M_3) = 220$ . Finally, after mentally switching to the motor  $M_0$  again, the subject with one mental action moved the motor to the desired region of the achievement motivation space, represented by the positive emoticon. The undesired region, which represents an unsuccessful outcome because of bumping into the obstacle, is represented with a corresponding negative emoticon.

#### B. Proof of the Concept Experiments

The number of subjects in the proof-of-the-concept experimental investigation was  $N = 10$ . Each subject had a training session consisting of two experiments. After the training, a subject carried out performance experiments which were used in statistical analysis. A total of 55 performance experiments were carried out. In 48 experiments the obstacle was avoided, so the success rate of this method was 87%. On average, an experiment lasted for 25.8 trials with a standard deviation of 6.1 trials.

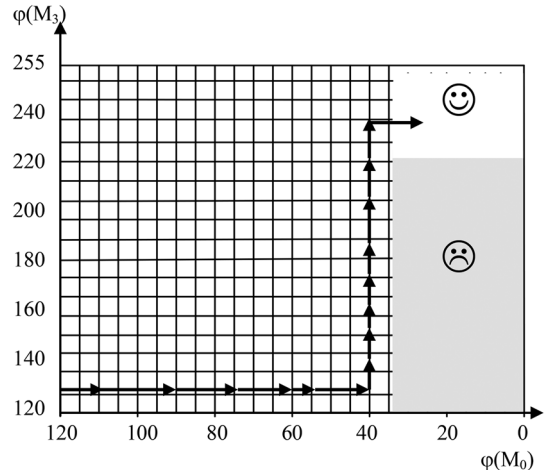


Fig. 17. The experiment from Table I shown in an achievement motivation space ( $\varphi(M_0)$ ,  $\varphi(M_3)$ ).

This proof-of-the-concept series of experiments confirmed the feasibility of the concept of the mentally emulated EEG demultiplexer. It also showed that a mentally emulated redundant demultiplexer can be used in solving tasks of EEG control of two physical devices by a single EEG channel. The methods implemented are scalable. They are based on the concept of an EEG message, in which several frames of information are encoded by a subject in a single EEG channel.

#### C. Beyond the Proof of the Concept

The EEG demultiplexer device (hardware + software) is applied in a research project on achievement motivation. The experiment described above is viewed as an EEG-based psychokinesis [23] experiment, in which a subject is building achievement motivation to achieve the EEG based psychokinesis task. The user of the EEG Demultiplexer application is the Biology Program of the South Carolina State University and the funding agency is the National Institute of Food and Agriculture.

The training of the subjects includes: 1) explanation about the generation of the alpha rhythm and relaxation techniques; 2) participation in biofeedback experiments where the heart rate and galvanic skin response are modulated using relaxation techniques; and 3) two training sessions in BRI before recording a BRI experiment.

The number of subjects that volunteered in this project is 49. Each subject was scheduled for a BRI session once a week for nine weeks. However, not all the subjects were able to have nine sessions and the total number of BRI experiments in which the EEG Demultiplexer was used was 352. The result of the study is out of the scope of this paper and will be reported by the user of the EEG Demultiplexer application. This is just to report that the system developed in this work is already an application.

## XII. DISCUSSION

This work looks into a somewhat overlooked topic in psychology and philosophy of the mind, namely the topic of mental action and the related topic of mental state. Using the association that digital circuits are based on the concepts of states and actions as transitions between states, this work considers the building of mentally emulated digital circuits, such as switches,

flip-flops, and demultiplexers. The *mental states have their EEG manifestations*, so the input signals to the considered as mentally emulated electronic circuits can be EEG signals. The discussion on mentally emulated devices such as switches and flip-flops is based on our previous works [18]–[23]. The new device proposed in this paper is the EEG demultiplexer.

The EEG demultiplexer introduces two theoretical concepts in relation to EEG manifestations and communications of the mental states, as well as in relation to BRI research.

The first concept is the EEG demultiplexer itself. It allows for sending of several commands to an external device through a single EEG channel. As pointed in [13]: “Inexpensive, noninvasive, and single-electrode EEG (electroencephalogram) technologies will play a key role in the following application areas: mind-controlled robots, drones, prosthetics, personal healthcare systems, smart homes, and smart hospitals/nursing-homes.” The EEG demultiplexer can be viewed as a response to the pointed Challenge.

The second concept is the *EEG modem* and viewing some brain rhythms (for example the EEG alpha rhythm) as amplitude modulation (AM) of a message to be sent from a mental state to outside the brain. Thus, the alpha rhythm is viewed not only as a manifestation of a particular mental state, but also as a modulation signal which can carry a message signal both inside and outside the brain. The modulation theory can therefore be used to build a BRI application, as shown in this work.

The field of Brain-Robot Interaction (BRI) passed a long way since 1988 [18], [19], when a simple mobile robot was controlled, to a 21st century control of humanoid robots [39]. The challenges still remain, whereas one of them is stated in [13] to build a single channel BRI, and another is pointed out in this paper as viewing EEG signals as modulation signals (chaotic [34] rather than harmonic) of messages from the brain.

A possible application in the computer industry is in electrophysiologically interactive computer systems [40]. An EEG demultiplexer enables EEG control of several devices using a single EEG channel, which offers a possibility to the computer industry to include the EEG inputs in products, including portable and wearable devices. The serial input might be a new device, a standard USB port, a serial wireless input, or an audio port.

### XIII. CONCLUSION

Following the motivation that understanding by building is a good approach towards understanding of the concepts of mental states, actions, and their EEG manifestations, this work developed a mentally emulated digital device, the EEG demultiplexer. The newly developed device extends the family of mentally emulated digital devices, which so far contained an EEG switch and a CNV flip-flop.

The EEG demultiplexer can be used in applications of Brain-Robot Interaction, for which this work has provided an experimental proof of that concept. A robot arm was controlled by an EEG demultiplexer in avoiding an obstacle on a trajectory towards a goal state.

The EEG demultiplexer is built, tested with proof-of-the-concept experiments, and then installed at a user site as an EEG Demultiplexer application where it was used in a project.

During the development of the EEG demultiplexer, two theoretical concepts were introduced in the EEG manifestations of mental states. One is the EEG demultiplexer itself, which allows for sending of more than one command to physical (or virtual) devices outside the brain using a single EEG channel. The method shown is potentially scalable to more commands.

The other concept is the EEG modem concept. It points out that EEG waveforms, in addition to being viewed as manifestations of mental states, can be considered as modulation signals which carry message signals from the brain over media inside and outside the brain. Indeed, in this paper the commands to the robot are demodulated from the EEG alpha rhythm.

Possible applications relevant for the computer industry are in a new generation of inputs for laptops and other portable and wearable devices, where in the near future a biosignal input might become a standard input interface.

This work contributes to the field of autonomous mental development by considering the concepts of mental states and actions, and showing applications of those concepts in building mental constructs such as mentally emulated digital circuits. It can be used as a framework for discussion on developing mental skills, such as a skill to control EEG signals emanated from a human brain as result of mental actions and states.

### REFERENCES

- [1] L. O'Brien and M. Soteriou, *Mental Actions*. London, U.K.: Oxford Univ. Press, 2009.
- [2] Wikipedia, “Mind. Mental Faculties,” Dec. 26, 2014.
- [3] M. Xie, *Fundamentals of Robotics: Linking pPerception to Action*. Singapore: World Scientific, 2003.
- [4] H. Lieberman, “Cognitive methods for assessing mental energy,” *Nutrit. Neurosci.*, vol. 10, no. 5–6, pp. 229–242, 2007.
- [5] G. Walter, R. Cooper, V. Aldridge, and W. McCallum, “Contingent negative variation: An electric sign of sensory-motor association and expectancy in the human brain,” *Nature*, vol. 203, pp. 380–384, 1964.
- [6] H. Berger, “Über das elektroencephalogramm des menschen,” *Arch. Psychiat. Nervenkr.*, vol. 87, pp. 527–570, 1929.
- [7] R. Pfanzner and W. McMulle, “Electroencephalography (EEG) I,” *Biopac Student Lab Manual*, Biopac Systems, 2013.
- [8] S. Palva and M. Palva, “New vistas for a-frequency band oscillations,” *Trends Neurosci.*, vol. 30, no. 4, pp. 150–158, 2007.
- [9] W. T. Blume, M. Kaibara, G. M. Holloway, and B. G. Young, “The Normal EEG in Children,” 2012 [Online]. Available: <http://icnapedia.org/wiki/clinical-neurophysiology/2774-the-normal-eeeg>
- [10] R. Pfeifer and C. Scheier, *Understanding Intelligence*. Cambridge, MA, USA: The MIT Press, 2000.
- [11] C. Canning and M. Scheutz, “Functional near-infrared spectroscopy in human robot interaction,” *J. Human-Robot Interact.*, vol. 2, no. 3, pp. 62–84, 2013.
- [12] J. Vidal, “Toward direct brain-computer communication,” *Annu. Rev. Biophys. Bioeng.*, pp. 157–180, 1973.
- [13] D. Aslam, “Mind-controlled robotics special call,” *Micromachines*, 2014 [Online]. Available: [http://www.mdpi.com/si/micromachines/mind-controlled\\_robotics](http://www.mdpi.com/si/micromachines/mind-controlled_robotics)
- [14] NeuroSky, EEG Biosensor Solutions 2014 [Online]. Available: <http://neurosky.com/products-markets/eeg-biosensors/>
- [15] R. Palaniappan, J. Gosalia, K. Revett, and A. Samraj, , A. Abaham, J. Muri, J. Buford, J. Suzuki, and S. Tampi, Eds., “PIN generation using single channel EEG biometrics,” in *Advances in Computing and Communication*. Berlin, Germany: Springer-Verlag, 2011, pt. Part IV, pp. 378–385.
- [16] A. Vyshedskiy, W. Kania, and R. Murphy, “Method and Apparatus for Physiological data Acquisition via Sound Input Port of Computing Device,” U.S. Patent US 2004/0220487 A1, 2004.
- [17] T. Lin and L. John, “Quantifying mental relaxation with EEG for use in computer games,” in *Proc. Int. Conf. Internet Comput.*, 2006, pp. 409–415.

- [18] S. Bozinovski, M. Sestakov, and L. Bozinovska, G. Harris and C. Walker, Eds., "Using EEG alpha rhythm to control a mobile robot," in *Proc 10th Annu. Conf. IEEE Eng. Med. Biol. Soc.*, New Orleans, LA, USA, 1988, vol. 3, pp. 1515–1516.
- [19] S. Bozinovski, O. Kaynak, Ed., "Mobile robot trajectory control: From fixed rails to direct bioelectric control," in *Proc IEEE Int. Workshop Intell. Motion Contr.*, 1990, vol. 2, pp. 463–467.
- [20] L. Soernmo and P. Laguna, *Bioelectrical Signal Processing in Cardiac and Neurological Applications*. New York, NY, USA: Academic Press, 2005.
- [21] L. Bozinovska, S. Bozinovski, and G. Stojanov, "Electroexpectogram: Experimental design and algorithms," in *Proc. IEEE Int. Biomed. Eng. Days*, Istanbul, 1992, pp. 58–60.
- [22] P. Sherz and S. Monk, *Practical Electronics for Inventors*. New York, NY, USA: McGraw-Hill, 2013.
- [23] S. Bozinovski, S. Markovski and M. Gusev, Eds., "Controlling robots using EEG signals, since 1988," in *ICT Innovations 2012*. Berlin, Germany: Springer-Verlag, 2012, pp. 1–11.
- [24] A. Craig, L. Kirkup, P. McIsaac, and A. Searle, S. Howard, J. Hammond, and G. Lindgaard, Eds., "The mind as a reliable switch: Challenges of rapidly controlling devices without prior learning," in *Human Computer Interaction*. London, U.K.: Chapman and Hall, 1997, pp. 4–10.
- [25] M. Barnes, "Switching devices and independence of disabled people," *Brit. Med. J.*, vol. 309, pp. 1181–1182, 1994.
- [26] A. Bozinovski, S. Tonkovic, V. Isgum, and L. Bozinovska, "Robot control using anticipatory brain potentials," *Automatika*, vol. 52, no. 1, pp. 20–30, 2011.
- [27] K. Addi, Z. Despotovic, D. Goeleven, and A. Rodic, "Modeling and analysis of a non-regular electronic circuit via a variational inequality formulation," *Appl. Math. Modeling*, vol. 35, no. 8, pp. 2172–2184, 2011.
- [28] Analog Devices, "AD8159–A 4-Lane 2:1 Multiplexer/Demultiplexer," 2005 [Online]. Available: <http://www.analog.com>
- [29] P. Kuekes, W. Robinett, G. Seroussi, and S. Williams, "Defect-tolerant interconnect to nanoelectronic circuits: Internally redundant demultiplexers based on Error-correcting Codes," *Nanotechnology*, vol. 16, no. 6, pp. 1419–1432, 2005.
- [30] Lynxmotion, "User Manual for SSC-32," 2006.
- [31] H. Jasper, "The ten twenty electrode system of the international federation," *Electroencephalography Clin. Neurophysiol.*, vol. 10, pp. 371–375, 1988.
- [32] N. Birbaumer, A. Kubler, N. Ghanayim, T. Hinterberger, J. Perelmouter, J. Kaiser, I. Iversen, B. Kotchoubey, N. Neumann, and H. Flor, "The thought translation device (TTD) for completely paralyzed patients," *IEEE Trans. Rehab. Eng.*, vol. 8, no. 2, pp. 190–193, Jun. 2000.
- [33] Emona Instruments PTY Ltd, "Envelope Recovery" Student Lab Manual," Dec. 26, 2014 [Online]. Available: [http://www.d.umn.edu/~sile0022/Experiment\\_5\\_%28Part\\_3%29.pdf](http://www.d.umn.edu/~sile0022/Experiment_5_%28Part_3%29.pdf)
- [34] A. Dmitriev, L. Kuzmin, and A. Laktushkin, "Amplitude modulation and demodulation of chaotic carriers," in *Proc. 12th Int. IEEE Workshop Nonlinear Dynamics Electron. Syst. (NDES'2004)*, Evora, Portugal, 2004, pp. 138–141.
- [35] Biopac. [Online]. Available: <http://www.biopac.com>
- [36] J. Atkinson, "Studies in projective measurement of achievement motivation," Doctoral Dissertation, University of Michigan, 1950, unpublished.
- [37] J. Atkinson, J. Atkinson and J. Raynor, Eds., "The mainsprings of achievement oriented activity," in *Motivation and Achievement*. Washington, DC, USA: Winston and Sons, 1974.
- [38] S. Bozinovski, M. Butz, O. Sigaud, and P. Gerard, Eds., in *Proc. Workshop Adapt. Behav. Anticipatory Learn. Syst.*, Edinburgh, U.K., 2002, pp. 100–119.
- [39] W. Li, C. Jaramillo, and Y. Li, "A brain computer interface based humanoid robot control system," in *Proc. IASTED Int. Conf. Robot.*, Pittsburgh, PA, USA, 2011, pp. 390–396.
- [40] J. Allanson, "Electrophysiologically interactive computer systems," *IEEE Comput. Mag.*, vol. 35, no. 3, pp. 60–65, Mar. 2002.



**Stevo Bozinovski** (M'81–SM'12) received the B.S., M.S., and Ph.D. degrees in computer science from the University of Zagreb, Zagreb, Croatia.

He is currently a Professor of Computer Science at South Carolina State University, Orangeburg, SC, USA. His previous experience includes IBM Deutschland in Bayreuth in Germany (1970–1973), Ricoh Hatano Plant in Hon-Atsugi in Japan (1984), University of Massachusetts at Amherst (1980–1981 and 1995–1996), and German National Center for Information Technologies (GMD) in Sankt Augustin in Germany (1999 and 2000). His research interests include brain–robot interaction, models of motivation–emotion in autonomous mental development, and interaction between learning and teaching systems.



**Adrijan Bozinovski** (M'09) received the B.S. in computer science from the University of Skopje, Skopje, Macedonia, and the M.S. and Ph.D. degrees in computer science from the University of Zagreb, Zagreb, Croatia.

Currently, he is an Assistant Professor in Computer Science at the University American College Skopje, Skopje, Macedonia. His research interests include brain–computer interactions, robotics, as well as algorithm design and analysis.